

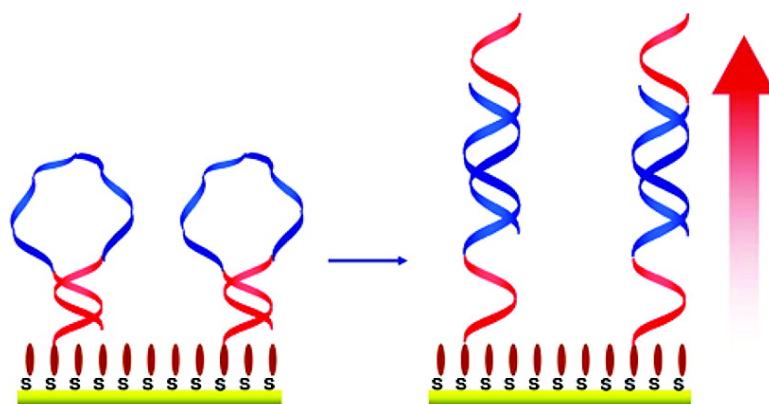
Article

Interfacial Behavior of a Hairpin DNA Probe Immobilized on Gold Surfaces

M. Steichen, N. Brouette, C. Buess-Herman, G. Fragneto, and M. Sferrazza

Langmuir, 2009, 25 (7), 4162-4167 • DOI: 10.1021/la802834a • Publication Date (Web): 13 February 2009

Downloaded from <http://pubs.acs.org> on April 16, 2009



More About This Article

Additional resources and features associated with this article are available within the HTML version:

- Supporting Information
- Access to high resolution figures
- Links to articles and content related to this article
- Copyright permission to reproduce figures and/or text from this article

[View the Full Text HTML](#)

Interfacial Behavior of a Hairpin DNA Probe Immobilized on Gold Surfaces[†]

M. Steichen,[‡] N. Brouette,[§] C. Buess-Herman,[‡] G. Fragneto,^{||} and M. Sferrazza^{*,§}

Service de Chimie Analytique et Chimie des Interfaces, Faculté des Sciences, Université Libre de Bruxelles, Boulevard du Triomphe, CP 255, 1050 Bruxelles, Belgique, Département de Physique, Faculté des Sciences, Université Libre de Bruxelles, Boulevard du Triomphe, CP 223, 1050 Bruxelles, Belgique, and ILL, Institute Max Von Laue Paul Langevin, Grenoble, France

Received August 29, 2008. Revised Manuscript Received January 28, 2009

Neutron reflection has been used in combination with electrochemical and quartz microbalance techniques to characterize a mixed monolayer of thiolated hairpin ss-DNA and 4-mercaptobutan-1-ol monolayer self-assembled on gold before and after hybridization with a cDNA target. Neutron reflection has revealed the opening of the stem-loop configuration of the probe associated with helix formation. This change in conformation correlates to the modification of the electron-transfer resistance associated with the $[\text{Fe}(\text{CN})_6]^{3-/4-}$ redox marker present in solution.

Introduction

The development of electrochemical DNA biosensors has gained increasing attention in the past decade because they offer promising alternatives to traditional techniques used to detect DNA hybridization.^{1,4} With the aim of developing sensitive and selective DNA biosensors on gold electrodes, much effort has been made to improve the DNA recognition layers on solid electrodes. Generally, these molecular layers consist of linear single-stranded oligonucleotide probes immobilized on a gold surface in order to recognize via hybridization the complementary target. However, DNA hairpin probes, presenting a stem-loop structure, have been shown to present several advantages over linear probes in terms of detection sensitivity and selectivity.^{5,9} Electrochemical DNA hybridization detection methods using hairpin DNA rely either on the presence of redox markers attached

to the 5' or 3' terminal of the DNA probe^{10,14} or on the use of unlabeled hairpin probes.^{15,18}

In a previous paper, we proposed for the first time the label-free electrochemical DNA hybridization detection of unlabeled hairpin DNA probes on gold by electrochemical impedance spectroscopy (EIS) in the presence of $[\text{Fe}(\text{CN})_6]^{3-/4-}$.¹⁵ More recently, electrochemical measurements involving unlabeled hairpin DNA on gold have been reported, showing that single-base mismatches can be successfully detected using these probes.^{16,18}

The hybridization of the end-tethered linear DNA probes to the complementary strand results in an increase in the distance of the DNA molecules from the surface as a result of the formation of the DNA double helix with a preferred orientation toward the surface normal. Such interfacial modification has already been probed by neutron reflectivity by Levicky et al.,¹⁹ who were able to determine the concentration profiles of self-assembled DNA monolayers containing linear oligonucleotide probes on gold before and after hybridization.

Neutron reflectivity (NR) has shown in fact to be a very sensitive profile analysis method in soft matter and biological work. Over the last 20 years, neutron reflection has emerged as a powerful technique for investigating surfaces and interfaces where detailed information on the concentration profile perpendicular to the sample can be obtained. The success of neutron reflection arises from the fact that, because of the short wavelengths available, it has a resolution on the angstrom level, so information is gained on the molecular level.²⁰ The technique is particularly useful for soft-matter studies because of the difference in scattering length density between hydrogen (H) and deuterium (D): by exchanging H with D in the material, the neutron refractive index can be modified, and a better contrast between different phases can be increased. This allows the use

[†] Part of the Neutron Reflectivity special issue.

* Corresponding author. E-mail: msferraz@ulb.ac.be.

[‡] Service de Chimie Analytique et Chimie des Interfaces, Université Libre de Bruxelles.

[§] Département de Physique, Université Libre de Bruxelles.

^{||} ILL.

(1) Sassolas, A.; Leca-Bouvier, B. D.; Blum, L. *J. Chem. Rev.* **2008**, *108*, 179–139.

(2) Lucarelli, F.; Tombelli, S.; Minunni, M.; Marrazza, G.; Mascini, M. *Anal. Chim. Acta* **2008**, *609*, 139.

(3) Palecek, E.; Scheller, F.; Wang, J., Eds. *Electrochemistry of Nucleic Acids and Proteins. Towards Sensors for Genomics and Proteomics*; Elsevier: Amsterdam, 2005.

(4) Odenthal, K. J.; Gooding, J. J. *Analyst* **2007**, *132*, 603–610.

(5) Kristin, B.; Cederquist, K. B.; Golightly, R. S.; Keating, C. D. *Langmuir* **2008**, *24*, 9162–9171.

(6) Pan, Q.; Zhang, R.; Bai, Y.; He, N.; Lu, Z. *Anal. Biochem.* **2008**, *375*, 179–186.

(7) Huang, T. J.; Liu, M.; Knight, L. D.; Grody, W. W.; Miller, J. F.; Ho, C.-M. *Nucleic Acids Res.* **2002**, *30*, 12.

(8) Wei, F.; Sun, B.; Liao, W.; Ouyang, J.; Zhao, X. *Sens. Bioelectron.* **2003**, *18*, 1149–1155.

(9) Trnková, L.; Postbieglová, I.; Holik, M. *Bioelectrochemistry* **2004**, *63*, 25–30.

(10) Fan, C.; Plaxco, K. W.; Heeger, A. J. *Proc. Natl. Acad. Sci. U.S.A.* **2003**, *100*, 9134–9137.

(11) Zauner, G.; Wang, Y.; Lavesa-Curto, M.; MacDonald, A.; Mayes, A. G.; Bowater, R. P.; Butt, J. N. *Analyst* **2005**, *130*, 345–349.

(12) Chatelain, G.; Chaix, C.; Brisset, H.; Moustrou, C.; Fages, F.; Mandrand, B. *Sens. Actuators, B* **2008**, *132*, 439.

(13) Xiao, Y.; Lai, R. Y.; Plaxco, K. W. *Nat. Protoc.* **2007**, *2*, 2875–2880.

(14) Xiao, Y.; Qu, X.; Plaxco, K. W.; Heeger, A. J. *J. Am. Chem. Soc.* **2007**, *129*, 11896–11897.

(15) Steichen, M.; Buess-Herman, C. *Electrochem. Commun.* **2005**, *7*, 416–420.

(16) Miranda-Castro, R.; de-Los-Santos-Alvarez, P.; Lobo-Castañón, M. J.; Miranda-Ordieres, A. J.; Tuñón-Blanco, P. *Anal. Chem.* **2007**, *79*, 4050–4055.

(17) Jin, Y.; Yao, X.; Liu, Q.; Li, J. *Biosens. Bioelectron.* **2007**, *22*, 1126–1130.

(18) Wang, Y.; Li, C.; Li, X.; Li, Y.; Kraatz, H.-B. *Anal. Chem.* **2008**, *80*, 2255–2260.

(19) Levicky, R.; Herne, T. M.; Tarlov, M. J.; Satija, S. K. *J. Am. Chem. Soc.* **1998**, *120*, 9787–9792.

(20) Fragneto, G. G. *J. Phys.: Condens Matter* **2001**, *13*, 4973.

of the contrast variation method, and different parts of the interface may be highlighted. For biophysics studies, a major advantage of reflectivity over other scattering techniques is that the required sample quantity is very small ($<10^{-6}$ g); therefore, it is suitable for work with expensive or rare macromolecules.

In this article, neutron reflectivity was used to show the biomolecular recognition process of unlabeled DNA hairpin probes, which induces a conformational change resulting in the opening of the stem-loop structure and the formation of rigid, rodlike duplex DNA. This conformational change causes a larger increase in the DNA layer thickness on the gold surface, as compared to that for layers composed by linear DNA probes. Electrochemical impedance and quartz crystal microbalance (QCM) measurements are directly correlated to the neutron reflectivity data.

Experimental Section

Chemicals and Sample Preparation. The DNA oligonucleotides are segments of the ARN 23S gene of *Helicobacter pylori*. They were purchased from Eurogentec (hairpin DNA probe: 5'-HS-(CH₂)₆-GTGAGC CAA GAC GGA AAG ACC C GCTCAC-3'; complementary target: 5'-G GGT CTT TCC GTC TT G-3'; noncomplementary sequence: 5'-C AGG AAA CAG CTA TGA-3'). The oligonucleotides were purified by RP-HPLC to remove failure sequences that could interfere during the experiments. A thiol-tethered probe oligonucleotide stock solution is prepared with a 10 mM phosphate buffer solution (pH 7.4) containing 1 mM EDTA and is kept frozen. Complementary and noncomplementary target oligonucleotides were dissolved in TE buffer (10 mM Tris-HCl, 1 mM EDTA, pH 7.4) and kept frozen for storage. The concentrations were determined by UV absorption spectroscopy. All solutions were prepared with ultrapure water from a Millipore Milli-Q system. 4-Mercaptobutan-1-ol from Fluka was stocked under argon at 4 °C. Potassium hexacyanoferrate (II/III) (Merck, Pro Analysis) was used as received. All chemicals were of analytical reagent grade.

The hairpin DNA probes were immobilized on the gold surface by forming mixed self-assembled monolayers of thiolated single-stranded oligonucleotides (HS-ssDNA) and a spacer thiol (4-mercaptobutan-1-ol, MCB) by spontaneous coadsorption. The DNA probes were mixed with MCB in a 1/1 molar fraction to obtain a total solution concentration of 50 μ M in 1.0 M potassium phosphate buffer (pH 7.4). The DNA_{hp}/MCB solution was placed on the cleaned gold surface overnight (>16 h) for self-assembly. The modified gold surface was finally rinsed with RB buffer (0.01 M Tris-HCl, 0.1 M NaCl, pH 7.4) and placed in the measurement cell.

Electrochemical Measurements. The electrochemical measurements were performed in a single-compartment cell connected to an Autolab PGSTAT 30 electrochemical analysis system with GPES and FRA 4.8 software (Eco Chemie). The three-electrode system consisted of a polycrystalline gold working electrode with a 1.6 mm diameter (Bioanalytical Systems), a large-area platinum electrode, and a reference electrode (Ag AgCl sat., Radiometer XR 300). All potentials are reported with respect to this reference electrode. The gold working electrode was polished with 1.0 and 0.05 μ m alumina-water slurry on a smooth polishing cloth. Afterwards, the electrode was ultrasonicated for 10 min and rinsed thoroughly with Milli-Q water. Finally, the electrode was electrochemically cleaned by cycling between potentials of -0.3 and $+1.5$ V in 0.1 M HClO₄ solution at a scan rate of 50 mV/s until reproducible cyclic voltammograms were recorded. The gold electrode was rinsed with Milli-Q water and dried for SAM modification. Supporting electrolytes were purged with nitrogen for at least 15 min before the experiments and kept under nitrogen during the measurements. Electrochemical impedance spectroscopy (EIS) measurements were carried out in a 0.01 M phosphate buffer solution (pH 7.4) in the presence of [Fe(CN)₆]^{3-/4-} (5×10^{-3} M, 1/1) at $+0.21$ V at $22(\pm 1)$ °C. A frequency range of 50 kHz to 50 mHz and an ac amplitude of 10 mV were applied.

Neutron Reflectivity Measurements. The NR measurements were performed at the Institut Laue-Langevin (ILL, Grenoble, France) using the D17 reflectometer. All NR experiments have been conducted in 0.01 M Tris-HCl buffer containing 1.0 M NaCl. It is assumed that the scattering length density ρ (SLD) of the solvents is not altered by the addition of the salts.¹⁹

The single-crystalline and (111) polished silicon substrate ($5 \times 5 \times 1$ cm³) was purchased from Siltronix (France). A thin chromium adhesion layer (5 nm) and a gold layer (14 nm) have been deposited by Cystec GmbH (Germany). The thicknesses of these layers were measured using spectroscopic ellipsometry prior to DNA adsorption. The resulting layers are sufficiently smooth for NR measurements.^{21,22} The samples were cleaned in a UV/O₃ chamber for 5 min prior to SAM adsorption.

The DNA_{hp}/MCB self-assembled layer was formed according to the same procedure as for the electrochemical measurements. The cell consists of two PTFE blocks that house the silicon block. In one of the blocks, there is a 4 cm³ cavity that allow the liquid to be in contact with the polished silicon surface. A full description of the cell is reported in refs 20 and 23.

The different steps of the sample preparation were characterized with neutron reflection and ellipsometry. First, the Si/SiO₂/Cr/Au substrate was characterized: the reflectivity profile for this system was fitted with a layer (box) model that includes the thickness, scattering length density, and roughness of the different layers. The values obtained from the fit of the thickness agreed with the values reported by the company that produced the Cr and Au deposition. The thickness of SiO₂ was also characterized before the deposition of Cr with ellipsometry, obtaining a value of 15 Å. The roughness extracted with NR was around 5 ± 2 Å for the different layers, as was also previously measured on silicon substrates.²⁴ Second, the MCB-monolayer was grafted, and we then characterized the Si/SiO₂/Cr/Au/MCB monolayer in the different contrast liquids. Again, a layer model was used. The thickness of the MCB monolayer obtained with NR is similar to the value obtained with ellipsometric measurements. The roughness of this monolayer is the same as that of the gold substrate. These two characterizations were essential for the experiments that followed: in particular, the parameters obtained for the thickness and SLD of the substrate layers were fixed for the fitting of the DNA systems. The DNA_{hp}/MCB self-assembled layer was directly formed on the gold substrate: short thiols, in our case MCB, are used as spacers so that hybridization is not hindered by the lack of accessibility of the probe. We stress that the DNA was terminally modified with a thiol linker (HS-(CH₂)₆-) to immobilize the DNA probe on gold. The thickness of this linker was close to that of the MCB layer (C₄ vs C₆). Using the parameters found for the Si/SiO₂/Cr/Au/MCB systems, we then fitted just the DNA layer (above the MCB spacers) using a layer model where only the thickness, the SLD, and the roughness of the DNA were changed before and after hybridization.

The concentration of DNA was around 1.2×10^{-11} mol/cm² as extracted with electrochemical measurements and 1.8×10^{-11} mol/cm² from NR, corresponding to around 2% of the total adsorbed amount on the surface.

Quartz Crystal Microbalance Measurements. QCM is a powerful technique that allows the quantification of very small adsorbed amounts (\sim ng/cm²) on a quartz crystal by measuring the frequency shift of a quartz piezoelectric resonator during adsorption experiments. The crystal is swept with different frequencies close to the quartz crystal's resonance frequency. The device is able to excite the system at different overtones. The frequency shift can be

(21) Burgess, I.; Zamylny, V.; Szymanski, G.; Schwan, A. L.; Faragher, R. J.; Lipkowski, J.; Majewski, J.; Satija, S. *J. Electroanal. Chem.* **2003**, *550–551*, 187–199.

(22) Zawisza, I.; Burgess, I.; Szymanski, G.; Lipkowski, J.; Majewski, J.; Satija, S. *J. Electrochim. Acta* **2004**, *49*, 3651–3664.

(23) Marsh, R. J.; Jones, R. A. L.; Sferrazza, M. *J. Colloid Interface Sci.* **1999**, *347*, 218.

(24) Carelli, C.; Jones, R. A. L.; Young, R. N.; Cubitt, R.; Krastev, R.; Gutberlet, T.; Dalglish, R.; Sferrazza, M. *Europhys. Lett.* **2005**, *71*, 763.

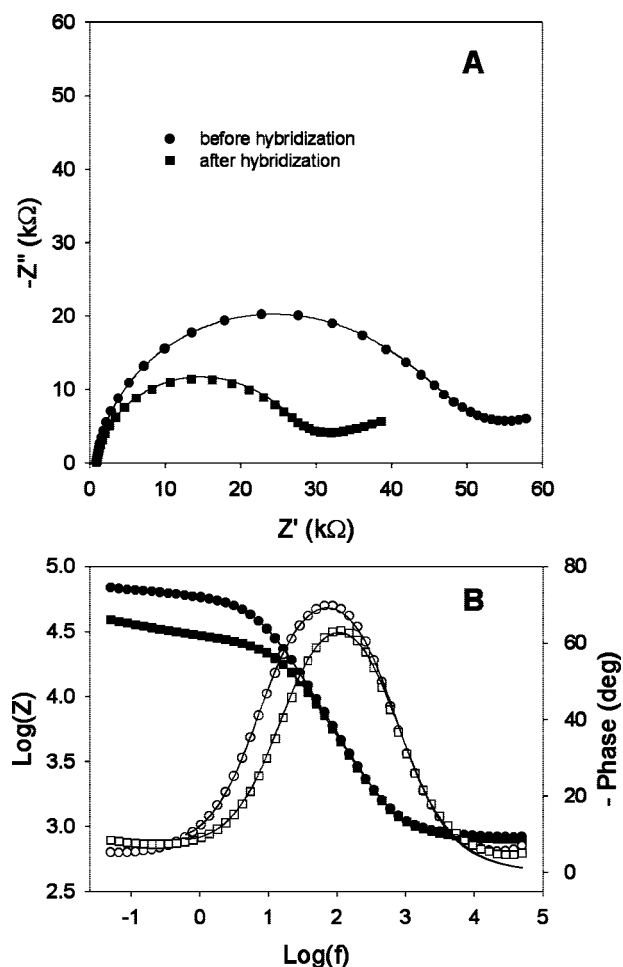


Figure 1. Impedance data of a hairpin DNA/MCB modified gold electrode before and after the addition of the 1 μM complementary strand. Impedance spectra (A) and Bode plot (B). (The Bode plot shows the phase angle (o) before and (\square) after hybridization and the logarithmic magnitude of the impedance (\bullet) before and (\blacksquare) after hybridization versus the logarithm of the frequency.) Measurements were performed in 0.01 M phosphate buffer (pH 7.4) in the presence of $[\text{Fe}(\text{CN})_6]^{3-/4-}$ (5 mM, 1/1) at + 0.21 V.

directly related to the adsorbed quantity by the Sauerbrey equation.²⁵ The QCM measurements were performed on the KSV QCM-Z500. The crystal used is a 5 MHz gold-coated quartz crystal sensor supplied by KSV. The crystal was cleaned with piranha solution (1/3 $\text{H}_2\text{O}_2/\text{H}_2\text{SO}_4$) for a couple of minutes and was thoroughly rinsed afterwards with ion-exchanged water. After being dried, the DNA_{hp}/MCB self-assembled layer were deposited as described earlier. The measurement chamber temperature was kept at 37.0 ± 0.3 °C.

Results and Discussion

The hybridization of the immobilized hairpin DNA probes resulting in a modification of the electrical properties of the interface was detected by electrochemical impedance spectroscopy in the presence of $[\text{Fe}(\text{CN})_6]^{3-/4-}$ as a redox couple in solution. Figure 1 shows the impedance spectra (A) and the Bode plot (B) of the DNA_{hp}/MCB modified gold electrode, respectively, before (\bullet) and after (\blacksquare) hybridization with the complementary target 16-mer sequence. The impedance spectrum is clearly modified when hybridization has taken place. For interfacial systems involving electron transfer, the classical Randles model is used to describe the impedance data.²⁶ In

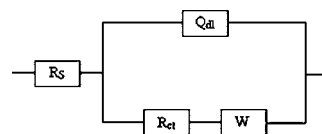


Figure 2. Equivalent circuit $R_s(Q_{dl}[R_{ct}W])$ used to fit the frequency scans with R_s being the solution resistance, R_{ct} being the resistance to charge transfer, Q_{dl} being a constant phase element modeling the double-layer capacitance, and W being the Warburg element.

addition to a resistance to charge transfer, a Warburg element is introduced to account for mass transfer. To take into consideration the deviation from ideal capacitance and diffusion behavior, a constant phase element is introduced into the Randles model. Its impedance is given by $Z_Q = (j\omega)^{-n}/Y_0$, where Y_0 is a proportionality constant depending on the characteristics of the electrochemical system. For $n = 1$, the constant phase element models a capacitance with $Y_0 = C$, and for $n = 0$, a resistance with $Y_0^{-1} = R$. For $n = 1/2$, a so-called Warburg element is observed that models semi-infinite diffusion.

The impedance data were fitted to the general equivalent $R_s(Q_{dl}[R_{ct}W])$ circuit (Figure 2). Fittings of data in Figure 1 are realized by considering frequencies from 50 mHz to 50 kHz. Table 1 gives the results of the fitting of the impedance data to the $R_s(Q_{dl}[R_{ct}W])$ circuit (Figure 2).

Because the Warburg element contribution is very small and $Z_{Q_{dl}}$ exhibits behavior close to that of an ideal capacity ($n = 1$), the data have also been fitted to a more simple equivalent circuit $R_s(Q_{dl}R_{ct})$ (Table 2), which is also in agreement with the analysis of Figure 1.

According to the two equivalent circuits considered, the fitting parameters clearly indicate that the electron-transfer resistance associated with the $[\text{Fe}(\text{CN})_6]^{3-/4-}$ redox marker present in solution decreases after hybridization. This effect can be correlated to the conformational change undergone by the DNA probe because the molecules lose their closed conformation and open upon hybridization. The electron transfer and diffusion of the redox marker is less hindered when the double helix is formed simply because of the reduced steric hindrance resulting from a less densely packed bilayer.

The main goal of the present work was to characterize the conformational change of the hairpin DNA probes after hybridization by an independent method in order to assess the electrochemical results.

Neutron reflection (NR), which was used successfully with linear DNA probes, was selected to probe the hybridization of hairpin DNA. The Si/SiO₂/Cr/Au substrate was modified by the MCB monolayer and has been characterized with NR in three different contrast liquids: H₂O, D₂O, and CMSi (this is a contrast liquid that matches the silicon scattering length density). From the fit using the layer model, the thicknesses d obtained were $d_{\text{SiO}_2} = 15 \pm 2$ Å, $d_{\text{Cr}} = 45 \pm 2$ Å, $d_{\text{Au}} = 141 \pm 5$ Å, and $d_{\text{MCB}} = 6 \pm 1$ Å. The thickness of SiO₂ was fixed to the value obtained with ellipsometry. For the scattering length density ρ , the following values were obtained: $\rho_{\text{Cr}} = 3.54 \times 10^{-6}$ Å⁻², $\rho_{\text{Au}} = 4.37 \times 10^{-6}$ Å⁻², and $\rho_{\text{MCB}} = -0.16 \times 10^{-6}$ Å⁻². For the scattering length density of Si and SiO₂, the values $\rho_{\text{Si}} = 2.07 \times 10^{-6}$ Å⁻² and $\rho_{\text{SiO}_2} = 3.45 \times 10^{-6}$ Å⁻² were used. The roughness of the different layers measured with NR for the Si/SiO₂/Cr/Au and Si/SiO₂/Cr/Au/MCB systems was around 5 ± 2 Å for all layers.

The large SLD contrast between MCB ($\rho = -0.16 \times 10^{-6}$ Å⁻²) and the D₂O bulk ($\rho = 6.35 \times 10^{-6}$ Å⁻²) allows us to well characterize the thickness of the MCB layer.

After the characterization of the substrate, the recognition layer DNA_{hp}/MCB is formed. The DNA is then characterized

(25) Sauerbrey, G. Z. Phys 1959, 155, 206–222.

(26) Randles, J. E. B. Discuss. Faraday Soc. 1947, 1, 11.

Table 1. Equivalent Circuit Parameters Fitted to the Circuit $R_S(Q_{dl}[R_{ct}W])$

	R_S (k Ω)	R_{ct} (k Ω)	Z_{Qdl} (Ω)		Z_W (10^{-4} Ω)
			Y_0 (10^{-6} S s n)	n	
before hybr.	0.838 (± 0.007)	56 (± 1)	0.53 (± 0.01)	0.918 (± 0.004)	0.9 (± 0.1)
after hybr.	0.810 (± 0.007)	27 (± 1)	0.60 (± 0.01)	0.905 (± 0.004)	1.3 (± 0.2)

Table 2. Fitting Parameters of the Equivalent Circuit $R_S(Q_{dl}R_{ct})$

	R_S (k Ω)	R_{ct} (k Ω)	Z_{Qdl} (Ω)	
			Y_0 (10^{-6} S s n)	n
before hybr.	0.833 (± 0.008)	59 (± 1)	0.57 (± 0.02)	0.909 (± 0.004)
after hybr.	0.804 (± 0.008)	28 (± 1)	0.67 (± 0.02)	0.889 (± 0.005)

using the three contrasts. During data analysis, the scattering length density values and the thickness of the substrate layers have been constant. It is reasonable to assume that the hybridization affects only the DNA probe layer. The results of the fit, using both a box model and a parabolic profile, indicate the presence of a DNA film with a thickness of around 50 ± 4 Å, with scattering length density of $\rho = 0.45 \times 10^{-6}$ Å $^{-2}$ (in H $_2$ O contrast). The SLD for the DNA varies linearly as a function of the quantity of D $_2$ O in the solution: $\rho = 3.4 \times 10^{-6}$ Å $^{-2}$ for H $_2$ O and $\rho = 4.3 \times 10^{-6}$ Å $^{-2}$ for D $_2$ O. This difference is connected to the exchange of H and D of the DNA amine groups. The quantity of water in the DNA layer can be estimated using the relation $\rho = \phi\rho_{\text{solv}} + (1 - \phi)\rho_{\text{DNA}}$, where ρ , ρ_{solv} , and ρ_{DNA} are the SLDs of the DNA harpin, of the solvent, and of the DNA, respectively. $(1 - \phi)$ is the volume fraction of the DNA layer. Considering the scattering length density obtained from the fits of the DNA layer in the three contrast fits ($\rho = 5.85 \times 10^{-6}$ Å $^{-2}$ for D $_2$ O, $\rho = 2.44 \times 10^{-6}$ Å $^{-2}$ for CMSi, and $\rho = 0.45 \times 10^{-6}$ Å $^{-2}$ for H $_2$ O), an estimation of the water content is $73 (\pm 5)\%$ for all three contrasts. The roughness of the layer is around 11 Å.

The solution TE buffer (10 mM Tris-HCl, 1 mM EDTA, pH 7.4) that contained 1 μ M complementary target oligonucleotides was added to the cell. The complementary DNA was then placed in contact with the DNAhp/MCB monolayer, and the system was heated to 37 °C for 2 h. After rinsing the cell with a solution of 0.01 M Tris-HCl/1 M NaCl/H $_2$ O, the three contrasts were measured at a temperature of 22 °C.

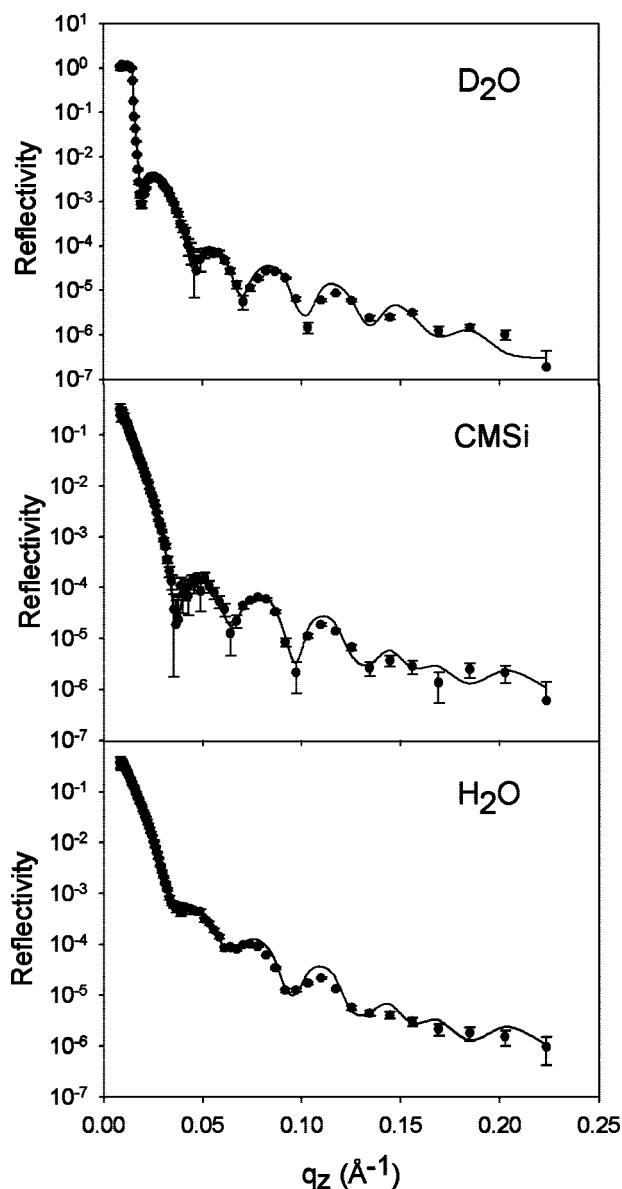
Figure 3 shows an example of the reflectivity after the hybridization process in the three contrasts: D $_2$ O, CMSi, and H $_2$ O from top to bottom, respectively.

Figure 4 shows a comparison of the H $_2$ O profile before and after the hybridization process: clearly the reflectivity profile changes after the biomolecular recognition process. The profile obtained by the fit is shown in the inset of Figure 4. With the addition of the cDNA, we can observe that the DNA thickness increases during hybridization: (90 ± 4) Å with a roughness of around (14 ± 4) Å.

On the basis of X-ray diffraction, the DNA oligonucleotide length can be estimated. For the DNA-B double helices, the distance between two close bases in the sequence is 3.4 Å. For linear DNA, this distance is 4.3 Å. In this way, an estimation of the length of the nucleotide chains can be obtained: around 45–55 Å for the stem-loop-structured DNA probe and 106 Å for the DNA helix after hybridization. Neutron reflection performed on a monolayer of linear DNA/MCH with comparable length showed a weaker change in the thickness of the monolayer after the insertion of the cDNA.¹⁹ The layer increased by 20 Å after helix formation for oligonucleotides of DNA with 25 bases. The larger increase at around 40 Å observed in our case can then be associated with the conformational change of the stem-loop-structured probes

toward a linear double-helical structure after hybridization, as illustrated in Figure 5.

The scattering length density of the layer is not modified significantly after the biomolecular recognition process, in agreement also with results of Levicky et al.¹⁹ The quantity of water considering the three profiles (D $_2$ O, H $_2$ O, and CMSi) is around $78 (\pm 4)\%$ for all three contrasts, similar to the water content observed previously. From the density profile, we can estimate the adsorbed quantity of DNA after the hybridization process. To first approximation, the De Feijter relation for the amount adsorbed (in mg/m 2) ($\Gamma_{\text{DNA}} = 0.1d\phi\rho_v$) can be used before and after hybridization.²³ In the expression, d is the thickness of the DNA monolayer in Å, ϕ is the volume fraction of DNA in the layer, and ρ_v is the density of DNA

**Figure 3.** Reflectivities profiles after hybridization in the three contrasts: D $_2$ O, CMSi, and H $_2$ O.

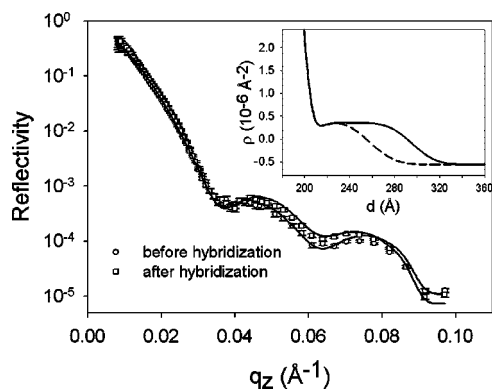


Figure 4. Reflectivity profile before (o) and after (□) hybridization in H_2O contrast. The lines are fit to the data. In the inset, the scattering length density profiles extracted by the fit are plotted: the dashed line is before and the continuous line is after the hybridization, showing the opening of the stem-loop configuration structure.

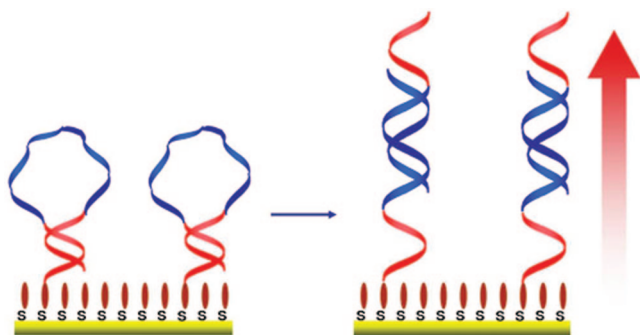


Figure 5. Sketch of the hybridization process after the insertion of cDNA.

in g/mL (estimated to be 1.7 g/mL). Considering the difference before and after the adsorption of cDNA, we can estimate the DNA excess in Γ_{DNA} to amount to $1.5 \pm 0.3 \text{ mg m}^{-2}$. This value was compared with the adsorbed amount extracted using QCM. In fact, the QCM technique was used to measure the amount of adsorbed cDNA during and after the hybridization process. The QCM crystal with the hairpin DNA monolayer was immersed in the buffer solution. After stabilization of the frequency, the cDNA target was inserted by a peristaltic pump into the measurement cell. The frequency shift was recorded as a function of time. When a plateau was reached, the DNA solution was replaced with the pure buffer, eventually to test the desorption process. Figure 6 (top) shows the QCM frequency shift for three different overtones (fifth, seventh, and ninth). We can observe that the hybridization process is very fast, with the frequency shifts reaching a constant plateau quite quickly. During rinsing, if we neglect the fluctuation connected to the injection of the liquid, no frequency shift is observed. Therefore, under these conditions, the hybridization process is totally irreversible.

Figure 6 (bottom) presents the adsorbed quantity due to hybridization calculated from the Sauerbrey equation.²⁵ All of the overtones give the same adsorbed amount, which is $2 \pm 0.2 \text{ mg/m}^2$. This quantity is in very good agreement with the adsorbed amount extracted from neutron reflection data. We have also performed a control experiment by inserting a non-cDNA molecule: in this case, no shift was observed as expected because no hybridization process takes place.

Conclusions

For DNA detection, electrochemical analysis is a promising tool because it presents several advantages over methods such

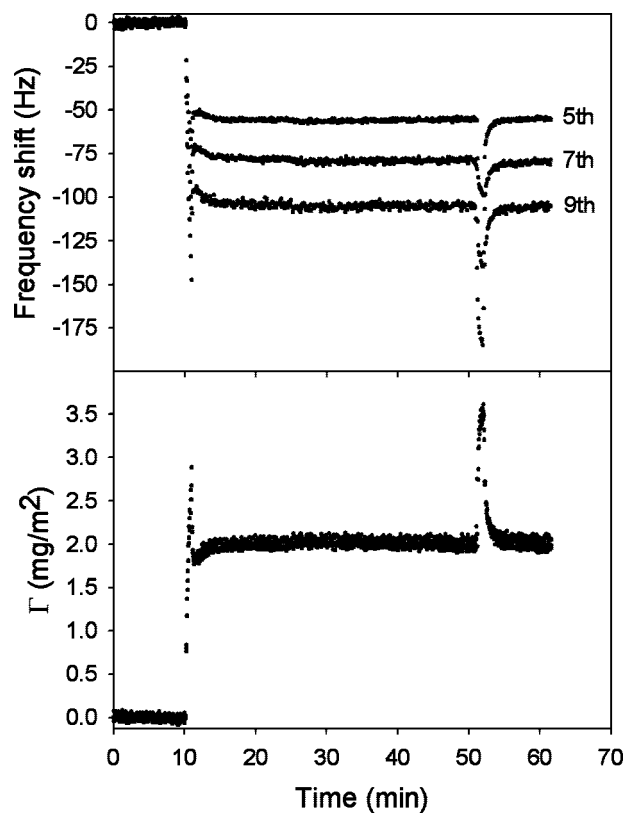


Figure 6. (Top) Frequency shift Δf for the fifth, seventh, and ninth overtones due to adsorption–hybridization by cDNA. We can observe the moment when cDNA is inserted (time = 10 min) and the time when the rinsing solution is inserted (time = 53 min). (Bottom) Adsorbed quantity Γ obtained by the Sauerbrey equation for the three overtones.

as fluorescence, for example, low cost, great sensitivity, and direct electronic readout. Moreover, electrical changes at the electrochemical interface can be detected without the need to label the target or probe with a redox center. In this work, we have confirmed by using neutron reflectivity that the modification of the impedance spectra, characteristic of the electrochemical interface, is directly related to the structural change of the DNA hairpin probe taking place after the hybridization of a hairpin DNA probe with a complementary unlabeled oligonucleotide sequence. The neutron reflectivity measurements have revealed the opening of the stem-loop configuration of the probe, which leads to helix formation associated with molecular recognition. This change is clearly more marked than the change in thickness of a linear DNA probe, as was reported earlier by Levicky et al.¹⁹ From the density profile, $1.5 \pm 0.3 \text{ mg m}^{-2}$ of adsorbed DNA within the mixed mercaptobutanol–DNA monolayer has been calculated, and this value is consistent with the adsorbed amount extracted from QCM data. Such values are expected because in order to ensure the specific interactions of the immobilized probes and to avoid the contribution of non-specifically adsorbed oligonucleotides the DNA probes are diluted in a matrix of shorter molecules. This is commonly achieved by a two-step procedure where the self-assembly of a thiolate–DNA monolayer is followed by its incubation in a solution of a short alkanethiol. We have shown here that a bioactive self-assembled mixed monolayer can be effectively formed in only one step consisting of the immersion of a gold surface in a mixed solution of thiolated ss-DNA and 4-mercaptobutan-1-ol. Finally, independent techniques such as neutron reflectivity and QCM have validated the electro-

chemical impedance change associated with the biomolecular recognition process and, as a result, the ability to use molecular beacons with electrochemical detection in the absence of redox labeling. Further studies will be focused on the recognition of DNA with proteins where conformational changes are of main importance for effective binding.

Acknowledgment. M.S. thanks the Fonds National de la Recherche Scientifique for a Research Fellow grant (Aspirant). This work was supported by an FNRC grant from the Belgium National Science Foundation.

LA802834A